International Conference on Mathematics, Computational Methods & Reactor Physics (M&C 2009)
Saratoga Springs, New York, May 3-7, 2009, on CD-ROM, American Nuclear Society, LaGrange Park, IL (2009)

A COMPARISON OF CONSTANT POWER DEPLETION ALGORITHMS

David C. Carpenter
Bettis Atomic Power Laboratory
P.O. Box 79, West Mifflin, PA 15122
carpente@bettis.gov

ABSTRACT

The depletion capability of the Common Monte Carlo Design Tool (CMCDT), under joint development at the Bettis and Knolls Atomic Power Laboratories, has been extended to include "constant power" depletion calculations. CMCDT couples the Monte Carlo transport code MC21 and depletion routines that use the VODE variable-coefficient ordinary differential equation solver. Three predictor-corrector "constant power" methods were implemented – the *cell2* and *monteburns* algorithms, which rely on constant flux computations, and a *linear rate* method that allows selected components of the coefficient matrix to change linearly during the depletion interval. Comparisons are made of these three coarse step methods against a reference depletion calculation of a 17 x 17 PWR assembly containing Gd-UO_2 fuel rods. The *linear rate* method gave consistently more accurate results, regardless of the size of the coarse timesteps and the level of spatial detail within the Gd-UO_2 fuel rods. All three methods have difficulty in modeling the fast rate of ^{157}Gd depletion with the *cell2* method having the most trouble.

Key Words: CMCDT, MC21, VODE, Constant Power Depletion

1. INTRODUCTION

The Common Monte Carlo Design Tool (CMCDT) is a joint development effort at the Bettis and Knolls Atomic Power Laboratories. The purpose of CMCDT is to provide an integrated environment for reactor design and analysis using the Monte Carlo transport solver MC21 [1] and several feedback modules. Depletion feedback is accomplished by the direct integration of MC21 with depletion routines that use the VODE [2] solution method. Depletion can be performed in either the traditional "constant flux" mode or with one of three predictor-corrector methods in "constant power" mode – the *cell2* method [3], the *monteburns* method [4], or a *linear* reaction *rate* change method (which has recently been implemented in the DRAGON suite of programs [5]). This report presents a comparison of these various methods. A brief description of the algorithms is presented in Section 2. Section 3 describes the physical model that was used for a 700-day depletion analysis of a quarter cell of a 17 x 17 PWR assembly that contains Gd-UO_2 fuel rods. Section 4 presents convergence analyses comparisons of fine timestep constant flux calculations and coarser timestep *linear rate* method solutions, establishing the timestep requirements for a suitable reference *linear rate* depletion calculation (5-day timesteps). Comparisons of the three constant power methods are given in Section 5. Each Gd-U fuel rod was modeled with a single depletion region. The *linear rate* method consistently provided the most accurate results for depletions with 10, 25 and 50-day timestep intervals; the *cell2* method generally provided the least accurate results. Section 6 demonstrates that these results still hold

when each Gd-U fuel rods is modeled with 10 depletable spatial rings. A potential drawback of this method is demonstrated in Section 7 while a discussion of how to improve the *linear rate* method is provided in Section 8.

2. CONSTANT POWER ALGORITHMS

The majority of depletion solvers assume a constant reaction rate during a specified burnup step. For multidimensional depletion analysis, errors are introduced with this constant reaction rate assumption since the actual flux levels and effective microscopic cross sections change both spatially and temporally during the burnup step to maintain a constant core power. To minimize the errors, depletion analysis would require a sequence involving a large number of small timestep depletion calculations. Although performing the depletions is fairly inexpensive, the real cost lies in the spatial calculations required to obtain the flux levels and effective cross sections for the depletion analysis. Consequently, employing a large number of timesteps becomes prohibitively expensive. To reduce the cost of depletion analysis, it is desirable to have coarse timestep calculations that can predict the small timestep behavior within acceptable limits. Predictor-corrector methods can provide the desired coarse timestep capability.

In the predictor-corrector method, a set of constant reaction rates is predicted that replaces beginning-of-timestep (BOT) reaction rate data to correct the depletion. Two of the three predictor-corrector methods identified previously, *cell2* and *monteburns*, can be used with any depletion solver (linearized chains, matrix operator method, ODE solvers, etc.), assuming the solution is performed in constant reaction rate mode. These methods are summarized as follows:

The *monteburns* predictor-corrector method is a simple three-step process:

1. Using BOT reaction rates, deplete for ½ of desired timestep,
2. Compute an “average” set of reaction rates by performing a spatial flux calculation with these intermediate set of number densities,
3. Redeplete over the full timestep using the corrected “average” reaction rates and BOT number densities. The resultant set of number densities become the initial conditions for the next timestep.

The *cell2* method is slightly more elaborate in that it involves one extra step:

1. Using BOT reaction rates, deplete for a full timestep
2. Compute the end-of-timestep (EOT) reaction rates by performing a spatial flux calculation
3. Redeplete over the full timestep using these EOT rates with BOT number densities,
4. For reaction rates that increase with time, the first depletion will underpredict the changes in nuclide concentrations while the second is thought to overpredict the changes. The average of the number densities resulting from the two depletions is used to initialize the densities for the next timestep.

Unlike linearized chains and matrix operator methods, multi-step ODE solvers allow higher order approximations to be used for modeling the reaction rate changes during a timestep. This is taken advantage of in another predictor-corrector method, the *linear rate* method. In this method a linear rate change between the BOT reaction rates and the predicted EOT rates is assumed. To

improve accuracy, the process can be repeated iteratively using successive, improved, EOT predictions. The *cell2* and *monteburns* methods are not iterative processes. To increase their accuracy, the size of the timestep must be reduced in the *monteburns* method while the *cell2* method can be improved by performing an additional corrector depletion with an improved estimate of the EOT reaction rates as discussed in Reference 6.

Whereas the *monteburns* and *cell2* methods are strictly wrapper algorithms, the *linear rate* method also requires modifications to the depletion solution algorithm itself. ODEs solve the first order form of an initial value problem,

$$\begin{aligned} \dot{\mathbf{y}} &= \mathbf{f}(t, \mathbf{y}), \quad t_0 \le t \le t_{final} \\ \mathbf{y}(t_0) &= \mathbf{y}_0 \end{aligned} \tag{1}$$

VODE solves the system of equations using a discrete, linear multi-step method which produces a sequence $\mathbf{y}_0, \mathbf{y}_1, \ldots, \mathbf{y}_s, \ldots$, of values of **y** which approximate the true solution **y**(t), (i.e., the number densities), at the discrete time values $t_0, t_1, \ldots, t_s, \ldots$. In practice, $t_0 = 0$. For stiff problems, VODE uses variable coefficient Backward Differentiation Formulas (BDFs) of order q, $1 \le q \le 5$, which have the following form:

$$\mathbf{y}_s = \sum_{i=1}^{q} \alpha_{si} \mathbf{y}_{s-i} + h_s \beta_{s0} \dot{\mathbf{y}}_s \,. \tag{2}$$

The coefficients α_{si} and β_{s0} are functions of the current and past stepsizes $h_s, h_{s-1}, \ldots, h_{s-q+1}$, $(h_s = t_s - t_{s-1})$.The function $\dot{\mathbf{y}} = \mathbf{f}(t, \mathbf{y})$ must be supplied by the depletion program that calls the VODE routines. For constant flux depletion problems, the function is simply the depletion system coefficient matrix, $\mathbf{A}(t_0)$, multiplied by $\mathbf{y}_s$. For constant power depletion problems using variable reaction rates, the function is modified such that the coefficient matrix is allowed to change at each subinterval, i.e, $\mathbf{A}(t_s)$. To obtain a time-dependent coefficient matrix, a linear change in BOT and predicted EOT reaction rates is assumed. A differential slope matrix is computed for each of the various neutron reaction rates that are being modeled (since decay modes do not change; entries in the slope matrix are set to zero for decay-only entries). For depletion step n, the differential slope matrix is computed as $\mathbf{M}_n = (\tilde{\mathbf{R}}_n - \mathbf{R}_{n-1}) / \Delta t_n$, where $\tilde{\mathbf{R}}_n$ denotes the predicted reaction rates for the current timestep and Δt_n is the length of the depletion step. Using the differential slope matrix, the user-supplied function is modified to be

$$\mathbf{f}(t_s, \mathbf{y}_s) = \left[\mathbf{A}(t_0) + \mathbf{M} t_s\right] \mathbf{y}_s \,. \tag{3}$$

For solution efficiency, a Jacobian matrix, $\mathbf{f}_y(t, \mathbf{y})$, must also be supplied. For depletion problems, this function is also the coefficient matrix so that the same differential slope correction is made for the linear rate constant power method.

Given these modifications to the depletion solver, the linear rate wrapper algorithm is:

1. Deplete over the full timestep in constant flux mode
2. Compute EOT reaction rates by performing a spatial flux calculation
3. Compute the differential slope matrix
4. Redeplete using Equation (3)

5. If desired, iterate by going back to step 2. Iterations may be stopped by a simple eigenvalue convergence test on the EOT spatials, or by simply specifying the maximum number of iterations.

3. MODEL DESCRIPTION

To assess the merits of the three predictor-corrector methods, all depletions were performed using CMCDT with the same cross section data sets so that any differences are strictly due to the depletion algorithms, not the spatial flux solver. The physics model is a two-dimensional quarter module of a 17 x 17 type PWR fuel design as specified in Reference 7. Each of the U fuel rods contains 6.5 w/o ^{235}U while the Gd-U rods contain 4.0 w/o ^{235}U and 10.0 w/o Gd_2O_3. The geometry laydown of the quarter assembly is shown in Figure 1. For these depletions, a 30-fission-product (with an additional lumped residual fission product), 14-actinide model was used to describe the UO_2 depletion. The fuel bearing regions in the Gd-U fuel rods were modeled as either one spatial region (Sections 4 and 5) or as 10 equally-spaced spatial rings (Section 6), each spatial region assigned a unique depletable composition. The fuel rods were given an edit region assignment for identification purposes as shown in Figure 1, the U-only fuel rods numbered before the Gd-U rods. All cross sections were evaluated at 73ºF. A constant energy per fission value of 201.2 MeV/fission was used for all fissionable nuclides. The spatial calculations at each step were run with 60 million active neutron histories. For each of the predictor-corrector methods, four sets of depletion histories were run based on maximum intervals of 10, 25, 50 or 100 days. The initial timesteps ramped up to the desired maximum step size using intervals of 2, 8, 10 or 15, 25, 50 and 100 days. The calculations were run out to a total of 700 days of depletion. The power density for all depletions was set at 37.5 W/gm of initial uranium loading. All results are based on a single realization of the depletion sequence; therefore, stochastic uncertainties in nuclide concentrations could not be assessed.

4. CONSTANT FLUX VS. THE LINEAR RATE METHOD

To achieve accurate solutions, all three constant power methods rely on obtaining good predictions of the microscopic reactions rates. If the rate of change is close to being linear, very good accuracy may be achieved using coarse timesteps. However, ^{155}Gd and ^{157}Gd exhibit a strong non-linear reaction rate behavior as these nuclides deplete rapidly midway through the 700 day period. An initial constant flux depletion using 1-day timesteps was performed (the first two timesteps were 12-hour steps to capture the buildup of ^{135}Xe better). For this depletion, all fuel rods, including those containing gadolinium, were modeled with a single spatial region, each assigned unique depletable compositions. Figure 2 shows the relative change in the microscopic capture rates in region 65 (see Figure 1) for ^{155}Gd and ^{157}Gd as well as some other important nuclides. This fuel rod exhibited the largest changes in reaction rates over the course of the depletion.

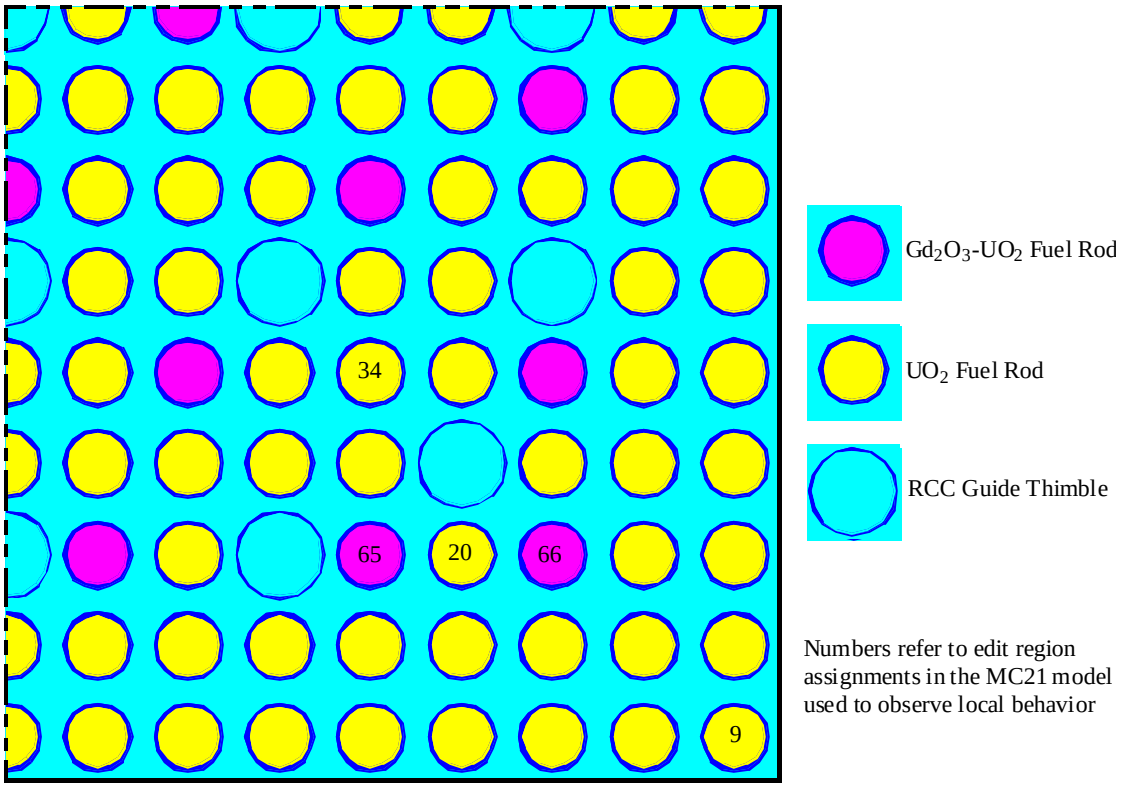

Figure 1. Geometry laydown of PWR quarter-assembly

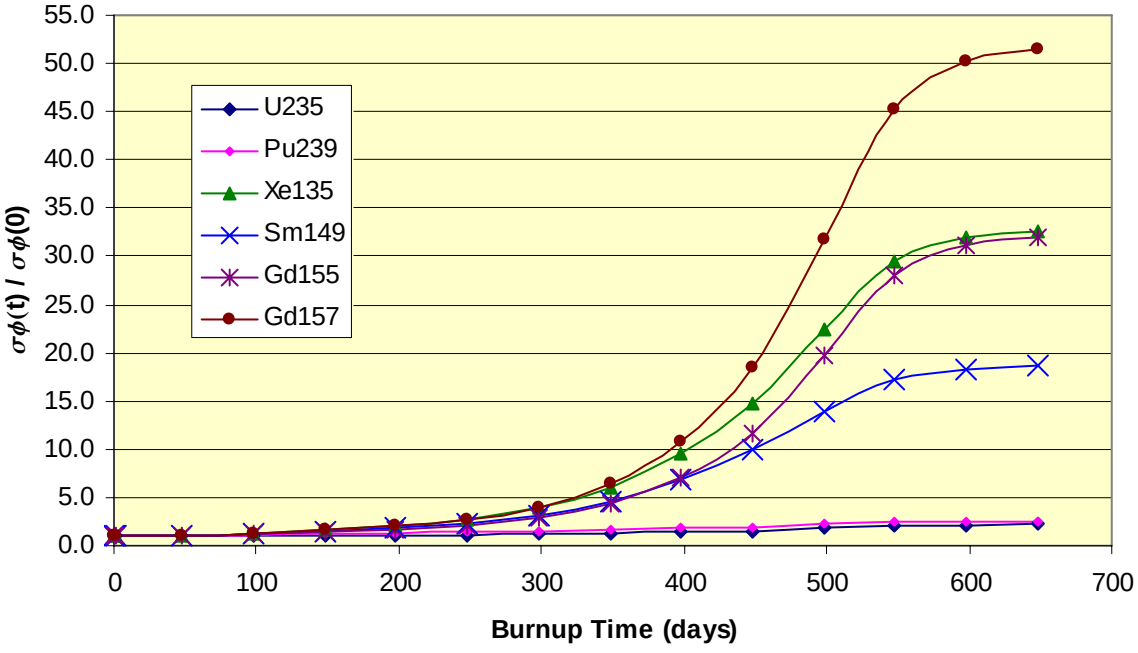

Figure 2. Relative change in microscopic capture rates for selected nuclides in region 65

The problem with using fine timestep constant flux calculations to establish a reference depletion is not knowing *a priori* how fine the time intervals should be. The usual practice to perform an error analysis is to repeat the depletion but with the timesteps reduced by a factor of two. A second depletion was run with 12-hour timesteps. Since the percent differences in concentrations relative to the 24-hour timestep depletion were significant, further refinements in timesteps were warranted. Redepleting the constant flux method with even finer steps over the full 700 day cycle was deemed too expensive and there was no guarantee that cutting the timesteps in half again would be sufficient. The period from 300 to 500 days exhibited the fastest rate of change in reaction rates and would be the hardest to capture correctly. Additional sensitivity analyses were performed just over this 200-day interval. Three constant flux depletions were run using fixed timesteps of 3, 12 and 48 hours. The initial conditions for all of these depletions used the concentrations from day 300 of the original 24-hour constant flux depletion.

Figure 3 shows the convergence trends in ^{157}Gd concentrations at various times throughout the 200-day constant flux depletions. The percent differences are relative to the 3-hour timestep solutions. Linear trend lines were projected to a timestep of size zero in order to predict the magnitude of the error that would exist in the 3-hour timestep solution. The maximum differences occur at 460 days. At this time period, the ^{157}Gd concentrations are low enough that they are now approaching a secular equilibrium with ^{156}Gd. All four of the depletions approach the same equilibrium value which is reflected by the 500 day curve showing smaller errors than the 450 day curve in Figure 3. Based on the projected differences, the 3-hour timestep solutions appear to overpredict the amount of ^{157}Gd remaining by a maximum of about 0.3%. A similar analysis was performed for a few other nuclides. The maximum projected error for ^{155}Gd is 0.1% while ^{135}Xe and ^{149}Sm are less than 0.05%. Depletion of ^{235}U is very accurate, with an expected error of less than 0.0005% using the 3-hour timestep intervals.

To establish the accuracy of the linear rate method, the 3-hour timestep constant flux solution can be used as a reference since the accuracy of that solution has been established. Two linear rate method depletions were run with 5- and 10-day timestep intervals. Figure 4 shows how well the ^{157}Gd concentrations from the linear rate solutions compare to the reference solution. Both of these calculations perform quite well, with maximum differences in ^{157}Gd concentrations well within 0.5% of the reference solution.

The cause of the negative trend in the 5-day timestep solution is a result of the linear rate method actually being more accurate than the constant flux reference solution, which, as discussed previously, slightly overpredicts the ^{157}Gd number density. This can be demonstrated using the same type of trend analysis that was used in the constant flux depletion analysis. Two additional linear rate depletions were performed using timestep intervals of 2.5 and 20 days. The resultant trend plots showed quadratic convergence behavior, but the statistical fluctuations in the data made it difficult to accurately project the fitted curves. Figure 5 shows the linear trend line behavior when the data is plotted as functions of the square of the timestep interval. It can be seen that the error made using the linear rate method using the 5-day timesteps is within 0.1% of the expected converged value.

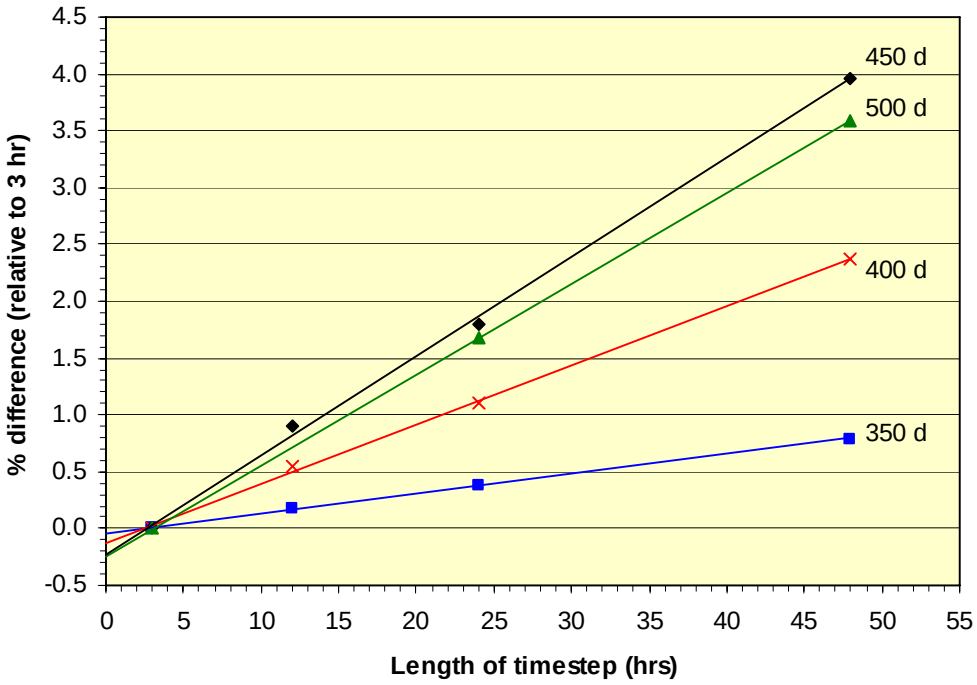

Figure 3. Convergence analysis of ^{157}Gd concentrations with constant flux depletions showing projected error of 3-hour solutions at various burnup times

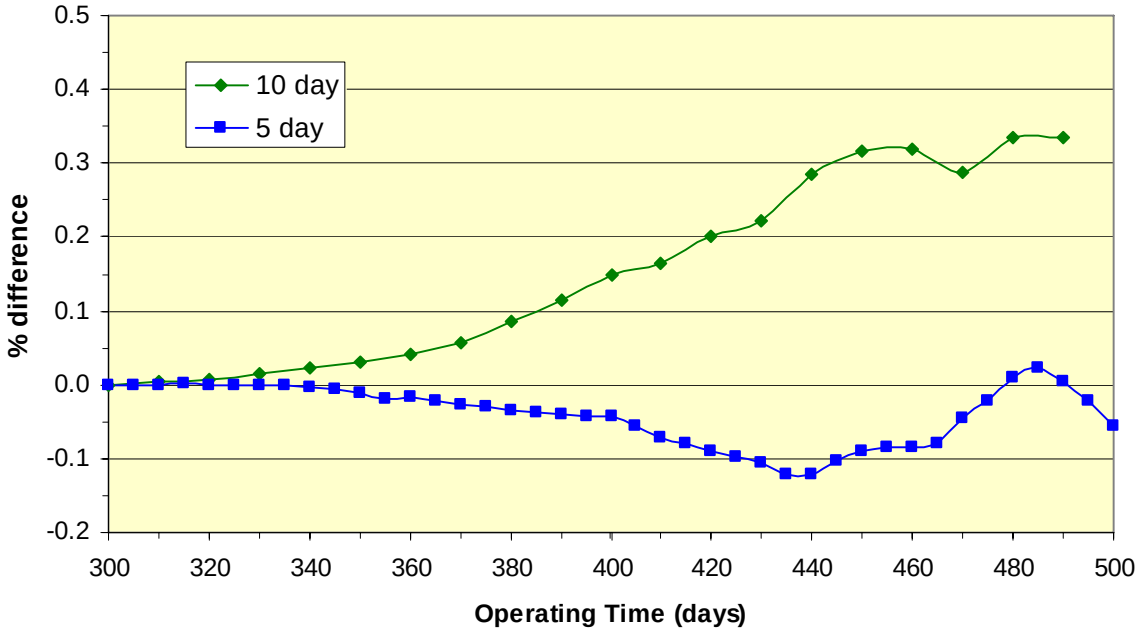

Figure 4. Percent difference in ^{157}Gd concentrations between *linear rate* constant power solutions and reference 3-hour constant flux solution

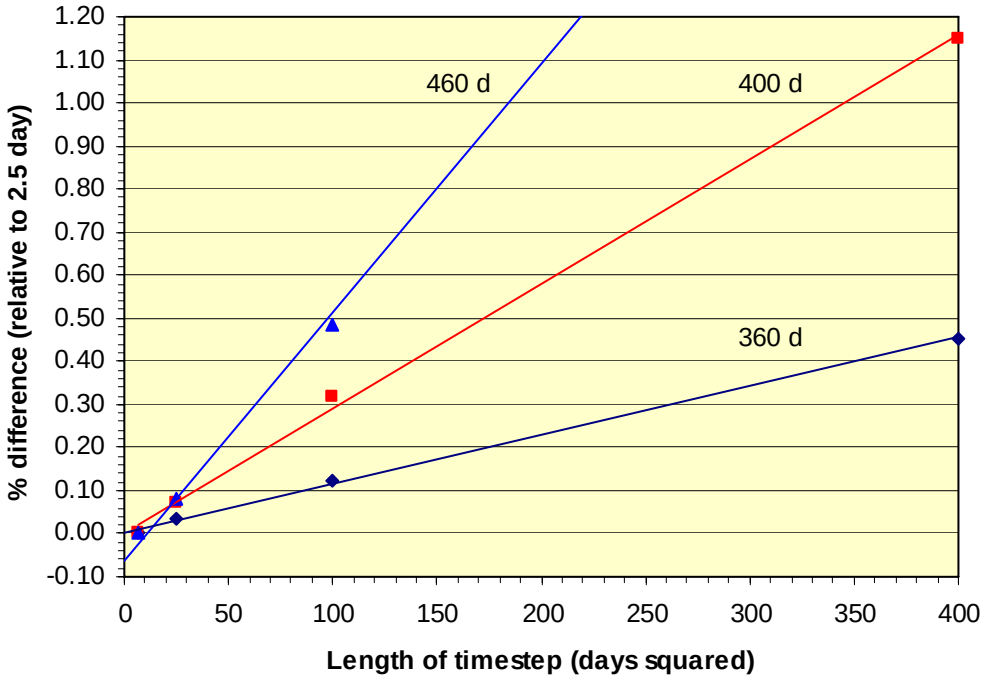

Figure 5. Convergence analysis of ^{157}Gd concentrations with *linear rate* depletions showing projected error of 2.5-day solutions at various burnup times

Using the Number Cruncher Statistical Systems (NCSS 2001) package [8], linear trend line analyses of the ^{157}Gd concentrations were performed for both the constant flux and linear rate method solutions at 20 day intervals from the 300 day starting point. The NCSS package computes the y-intercept which gives an indication of the "converged" solution. Table I shows these projected "converged" solutions at the various time sequences using linear regression analysis (the linear rate data used the square of the timestep intervals as the independent variable). The last column gives the percent difference between the constant flux and linear rate solutions. The accuracy that is obtained is much smaller than any differences that would be expected as uncertainties in nuclide concentrations and demonstrates that the linear rate constant power method and constant flux solutions can converge to the same solution provided the timestep lengths are sufficiently refined. This analysis verifies the proper operation of the linear rate method.

TABLE I. "Converged" ^{157}Gd concentrations (Region 65) at various depletion times based on linear trend projections

Depletion Time (days)	Constant Flux	Linear Rate	% Diff
320	2.220786e+20	2.220776e+20	-0.0005
340	1.584377e+20	1.584386e+20	0.0006
360	1.069017e+20	1.068942e+20	0.0070
380	6.772557e+19	6.771994e+19	-0.0083
400	4.022793e+19	4.022664e+19	-0.0032
420	2.265336e+19	2.265039e+19	-0.0131
440	1.247043e+19	1.247056e+19	0.0010
460	7.067616e+18	7.067888e+18	0.0038
480	4.346128e+18	4.347736e+18	0.0370

5. COMPARISONS OF THE CONSTANT POWER METHODS

The previous section demonstrates that both the 2.5-day and 5-day timestep *linear rate* method solutions were in close agreement and more accurate than a constant flux solution using 3-hour timesteps. For depletions over the full 700 day cycle, it would be too costly to use constant flux depletions to obtain the best reference solution. For purposes of the remaining study, using 5-day timesteps with the linear rate method is both cost effective and sufficiently accurate to perform an assessment of the three constant power algorithms. The final reference solution used in the following analyses used 5-day intervals over the full 700 days (the first four step intervals were 1, 2, 3, and 4 days). The coarse-step depletions were based on maximum time intervals of 10, 25, and 50 days. The initial timesteps ramped up to the maximum size using intervals of 2, 8, 10 or 15, 25, and 50 days, as required. As in the previous section, the Gd-U fuel rods are represented with just a single depletable composition.

Figure 6 shows the k_{eff} difference of the various coarse step depletions relative to this reference solution. Regardless of timestep size, the *linear rate* method exhibits the more accurate prediction. Statistical agreement in the k_{eff} difference was achieved between all three methods only when the timestep size was shortened to 10 days.

Figure 7 demonstrates that the *linear rate* method is at least twice as accurate as the *cell2* method in predicting ^{157}Gd for a given timestep size while the accuracy of the *monteburns* method falls somewhere in between the other two methods. At 10-day intervals, all three methods have nearly identical accuracy, with the *linear rate* method still having a slight edge in accuracy.

There are essentially no differences in total ^{155}Gd concentrations between the *monteburns* and *linear rate* methods irrespective of the size of the timestep as seen in Figure 8. The *cell2* method always has a higher error in its prediction. As before, all three methods are in close agreement when the timesteps are shortened to 10-day intervals.

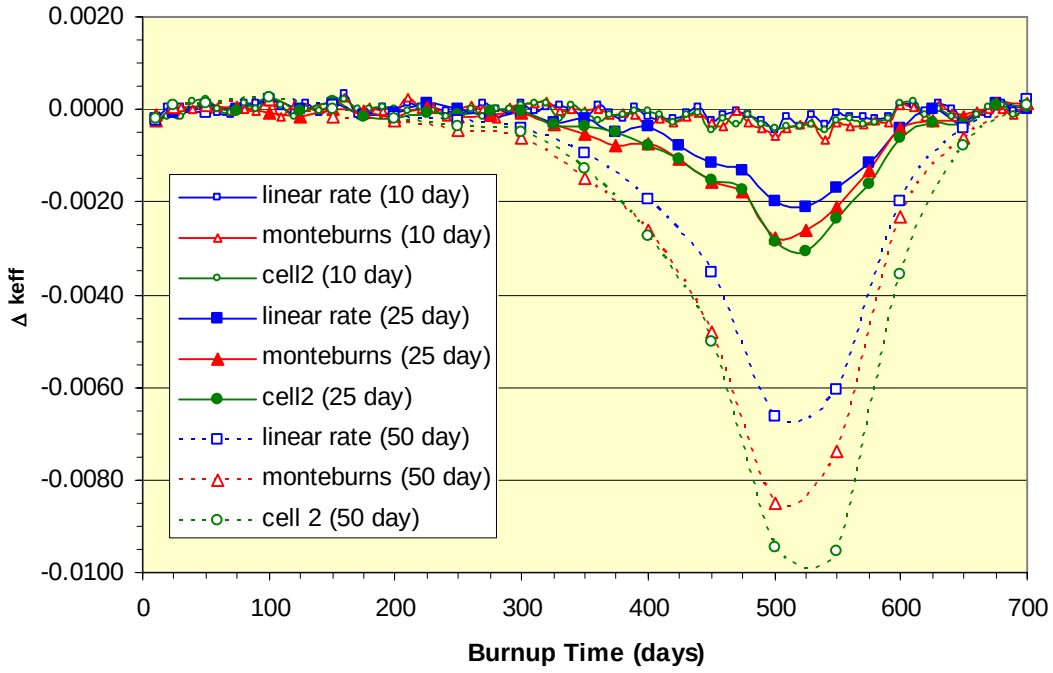

Figure 6. Difference in k_{eff} relative to the reference *linear rate* depletion (maximum size of timestep in parentheses)

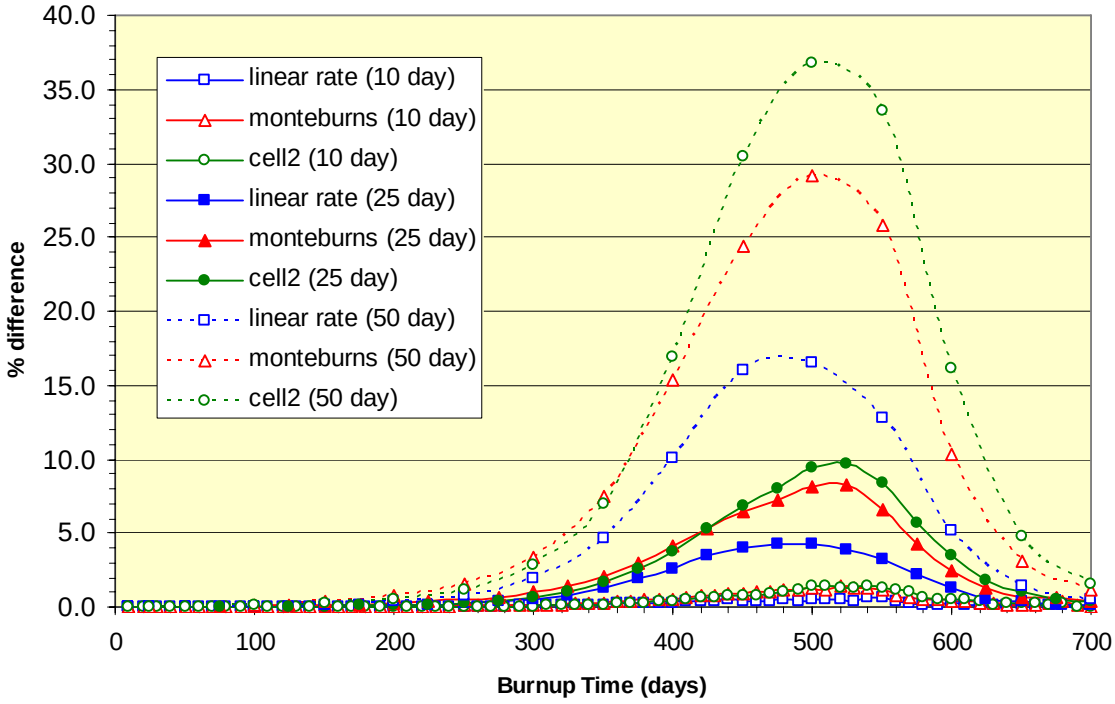

Figure 7. Percent Difference in ^{157}Gd Concentrations Relative to Reference Depletion

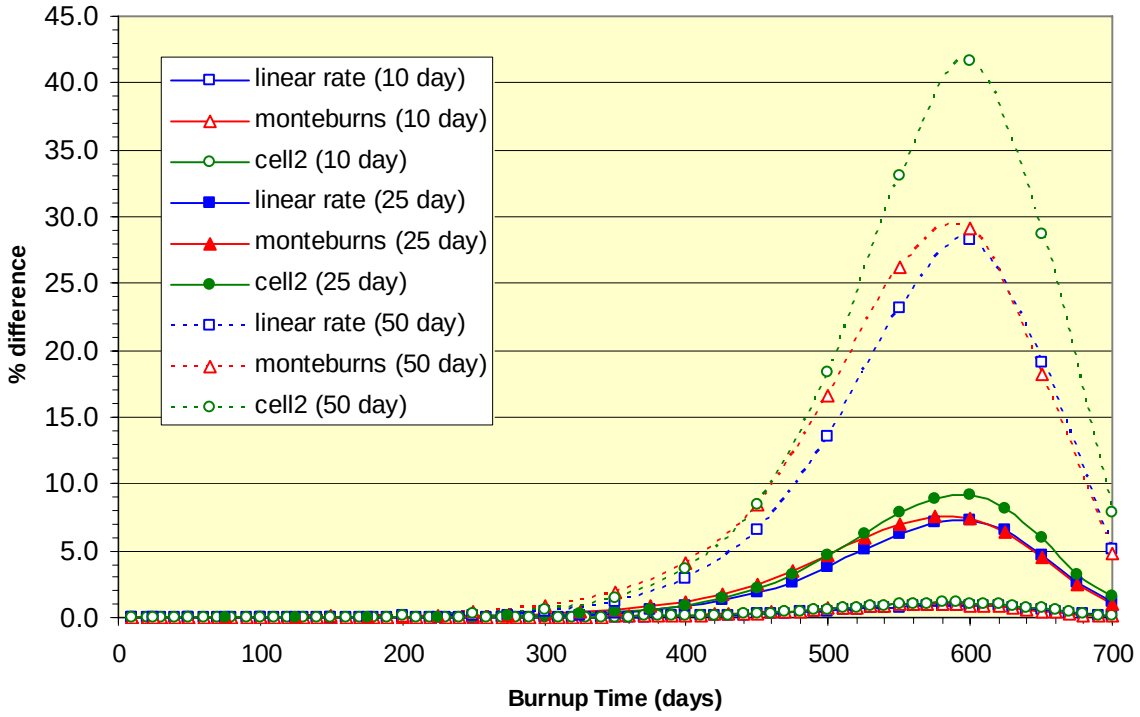

Figure 8. Percent Difference in ^{155}Gd Concentrations Relative to Reference Depletion

Although the reactivity differences seen in Figure 6 are initially driven by the differences in ^{157}Gd concentrations, the maximum reactivity differences are due predominately by differences in the ^{155}Gd concentrations. Using the 50-day timestep depletions, absorption fractions for these two nuclides were compared against the reference solution. These comparisons are shown in Table II. The absorption fractions that are given were obtained from the reference depletion. The values listed under the different predictor-corrector methods are the observed differences in the absorption fractions as a result of the error being made in the Gd concentrations.

TABLE II. Observed differences in ^{155}Gd and ^{157}Gd absorption fractions with 50-day timestep depletion

Burnup Time (days)	Nuclide	Absorption Fraction	*linear rate*	*monteburns*	*cell2*
400	^{155}Gd	0.07471	-0.00027	-0.00041	-0.00080
	^{157}Gd	0.01838	0.00132	0.00201	0.00235
450	^{155}Gd	0.06766	0.00129	0.00149	0.00126
	^{157}Gd	0.00680	0.00078	0.00122	0.00165
500	^{155}Gd	0.04493	0.00351	0.00403	0.00439
	^{157}Gd	0.00390	0.00036	0.00076	0.00099
550	^{155}Gd	0.01821	0.00349	0.00374	0.00482
	^{157}Gd	0.00346	0.00023	0.00061	0.00081
600	^{155}Gd	0.00507	0.00128	0.00127	0.00186
	^{157}Gd	0.00335	0.00009	0.00025	0.00039

The constant power methods demonstrate a wide range of accuracies in predicting the concentrations of the remaining depletable nuclides. These discrepancies are caused one way or another by the inaccuracy in calculating the Gd depletion. The coarser solution does not deplete ^{155}Gd and ^{157}Gd fast enough. As such, the actinide absorptions in the Gd-U fuel rods are too low (due to the higher absorption in the Gd isotopes) causing the fuel depletion to lag, resulting in higher concentrations of the actinides in those fuel rods (Figures 9-12). The fission rates in the Gd-U rods are also too low for the same reason. The differences observed in the short lived fission products which are essentially in equilibrium based on the local fission rate (e.g. ^{149}Pm, Figure 14), demonstrates that behavior. Both ^{135}Xe and ^{149}Sm have significant thermal absorption cross sections and compete for the same thermal neutrons as the Gd nuclides. Because of the high Gd concentrations, the absorption rates in ^{135}Xe and ^{149}Sm are reduced, resulting in larger inventories (Figures 13 and 15). The short-lived nature of ^{135}Xe is also affected by the opposing trend of ^{135}I (which behaves similarly to ^{149}Pm), much more so than the stable ^{149}Sm being affected by the opposing trend of ^{149}Pm.

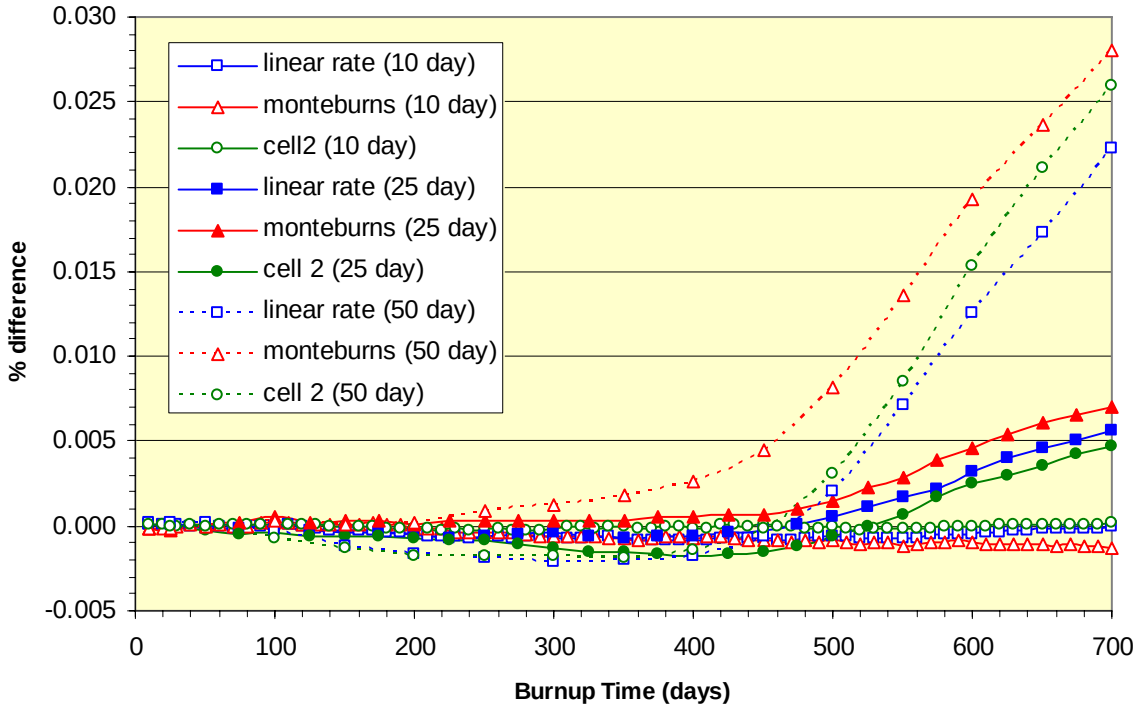

Figure 9. Percent Difference in ^{235}U Concentrations Relative to Reference Depletion

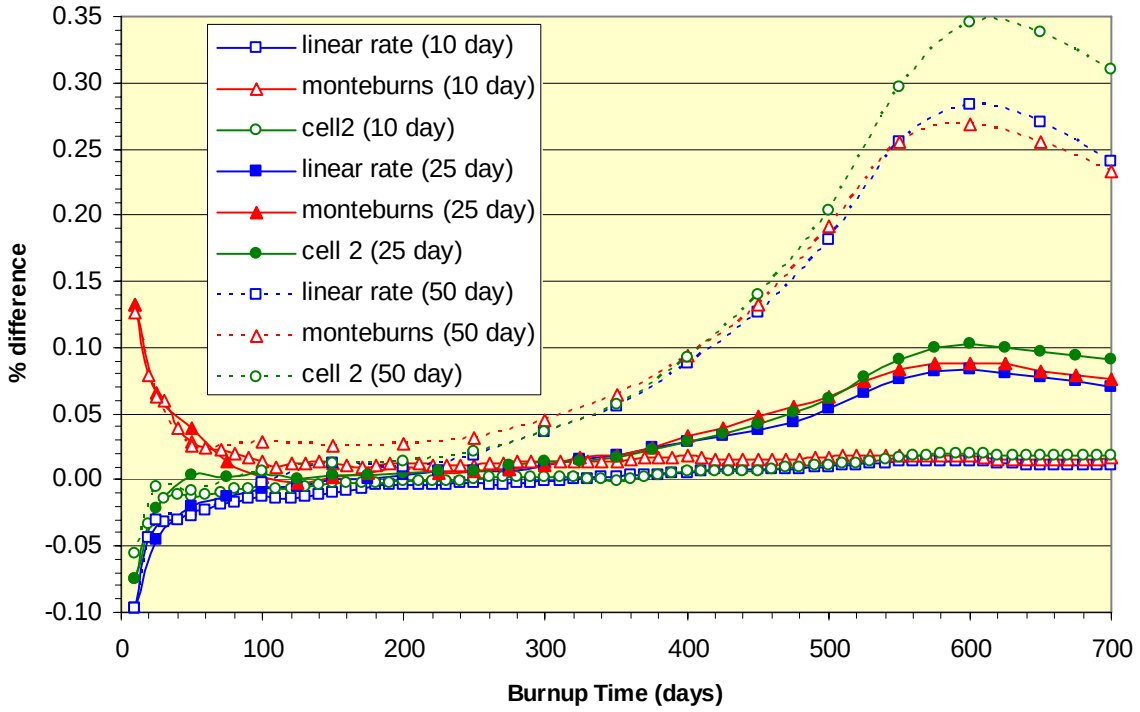

Figure 10. Percent Difference in ^{239}Pu Concentrations Relative to Reference Depletion

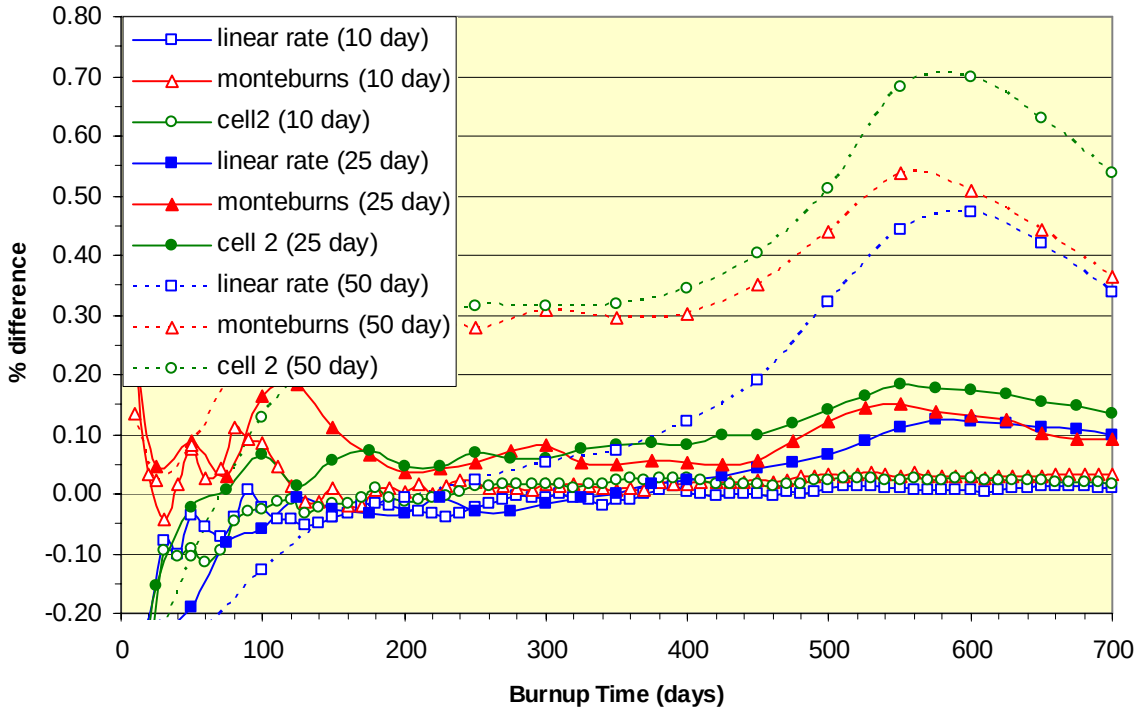

Figure 11. Percent Difference in ^{241}Pu Concentrations Relative to Reference Depletion

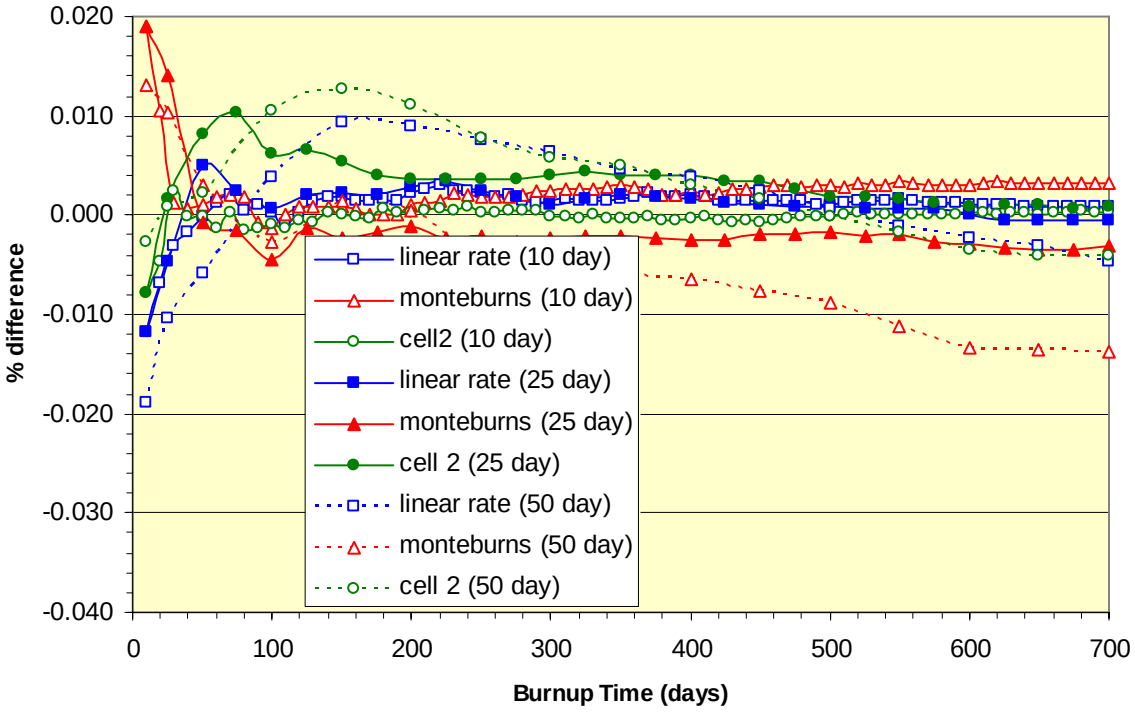

Figure 12. Percent Difference in the Fission Counter Relative to Reference Depletion

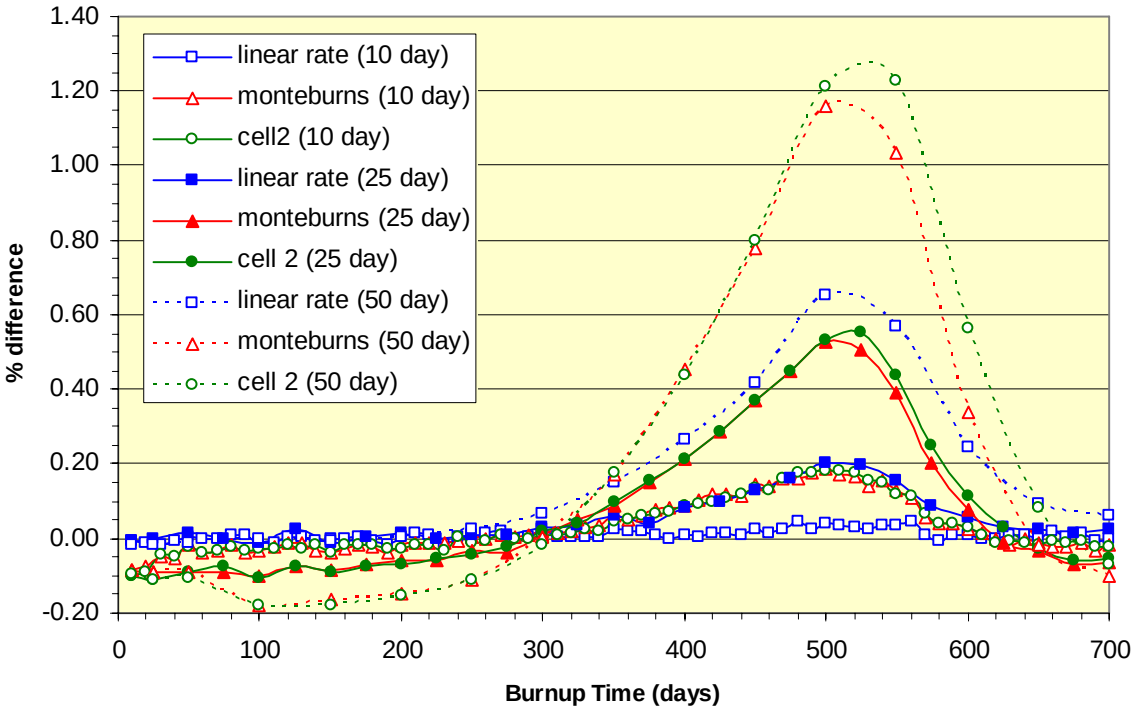

Figure 13. Percent Difference in ^{135}Xe Concentrations Relative to Reference Depletion

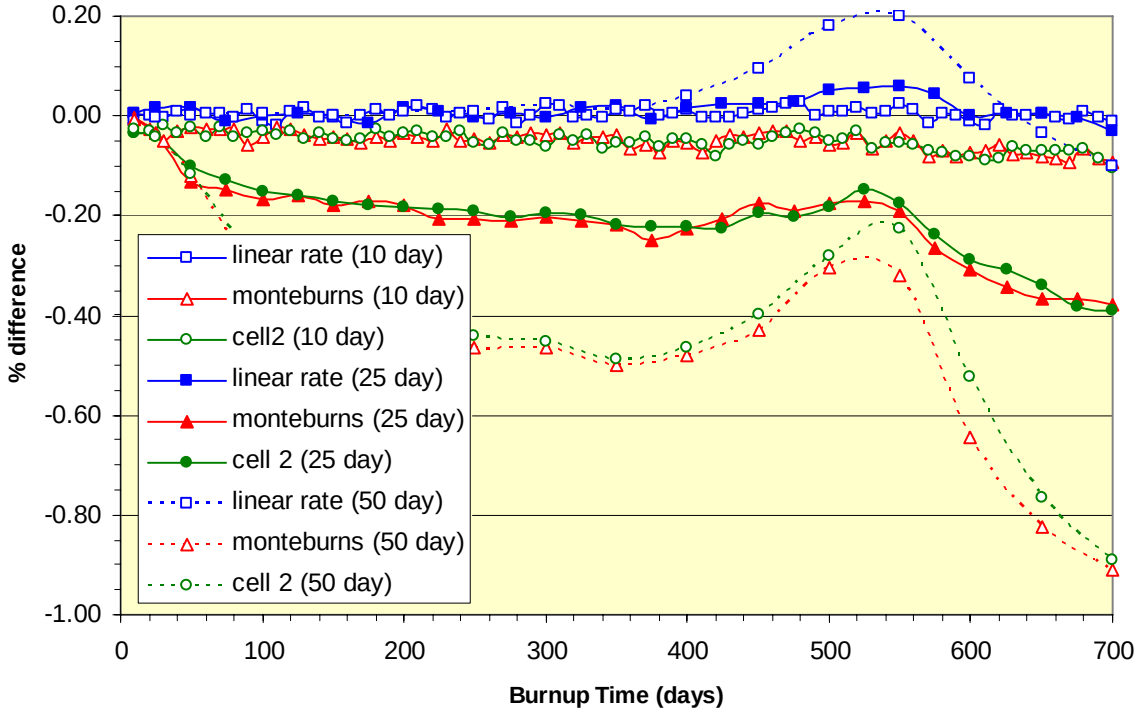

Figure 14. Percent Difference in ^{149}Pm Concentrations Relative to Reference Depletion

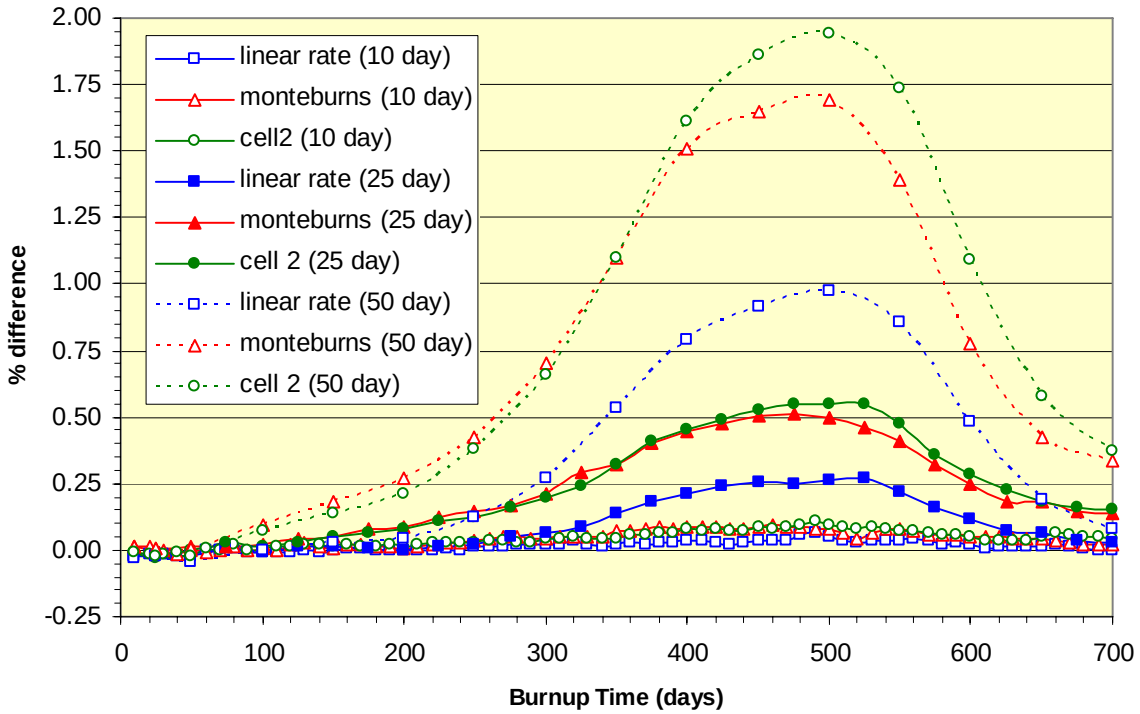

Figure 15. Percent Difference in ^{149}Sm Concentrations Relative to Reference Depletion

6. COMPARISONS WITH SPATIAL REFINEMENT

Gadolinium exhibits strong spatial self shielding which necessitates spatial refinement for accuracy in the depletion calculations. Each of the Gd-U fuel rods were divided into 10 equally spaced concentric rings. As before, a reference depletion was obtained using the *linear rate* method with the 5-day timestep intervals. All three methods were then redepleted using 10, 25 and 50 day intervals.

Figure 16 shows how well the three constant power methods predict k_{eff}. The *linear rate* and *monteburns* methods are very close in their predictions of k_{eff}, regardless of the size of the timestep. The *cell2* method is not as accurate and shows an increasing amount of error as the timestep length is increased.

Comparing these results with those shown in Figure 6, one will note that the level of accuracy with any of the methods has decreased when the Gd-U fuel rods are modeled with spatial detail. This is attributable to the change in gadolinium depletion characteristics when more interior detail is added. Figure 17 compares the total ^{155}Gd and ^{157}Gd concentrations in region 65 (see Figure 1) when modeled as either a single region or as 10 concentric rings. Note that adding the spatial detail will allow more Gd to be retained in the system much later in the depletion cycle. Figures 18 and 19 show how well the three constant power methods predict the total gadolinium concentrations relative to the reference solution. As with the 1-region results, the *cell2* method is the least accurate of the three.

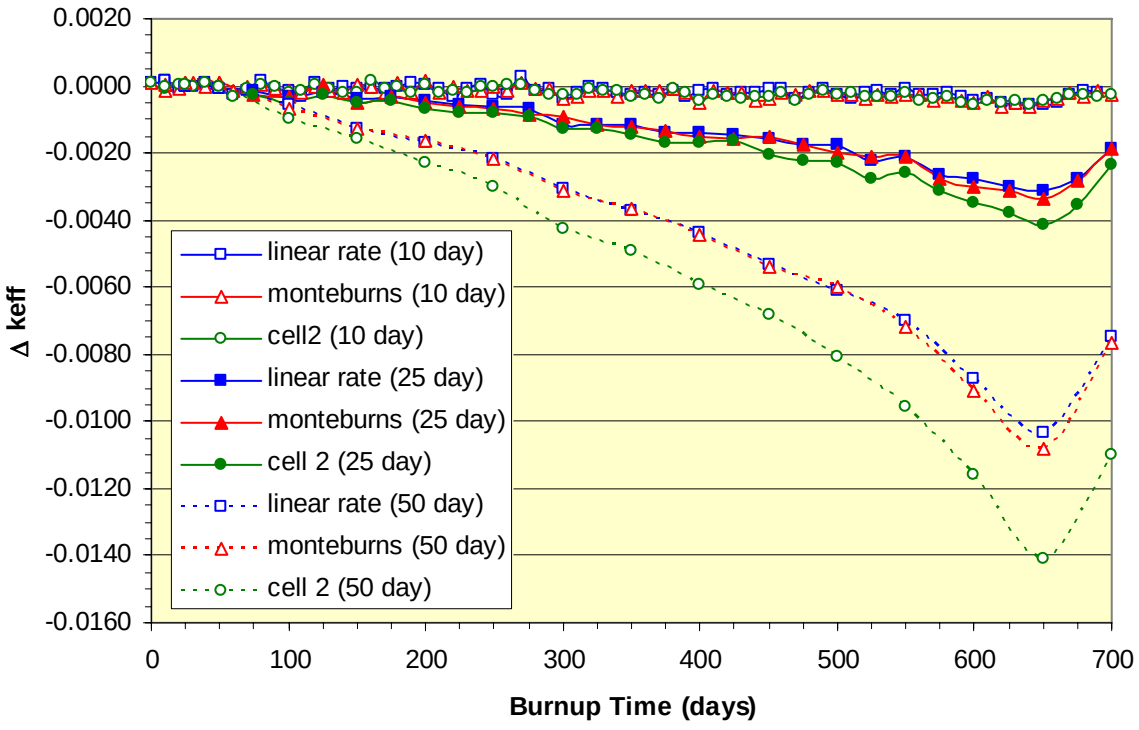

Figure 16. Difference in k_{eff} relative to the reference *linear rate* depletion using 10-region Gd-U fuel rods

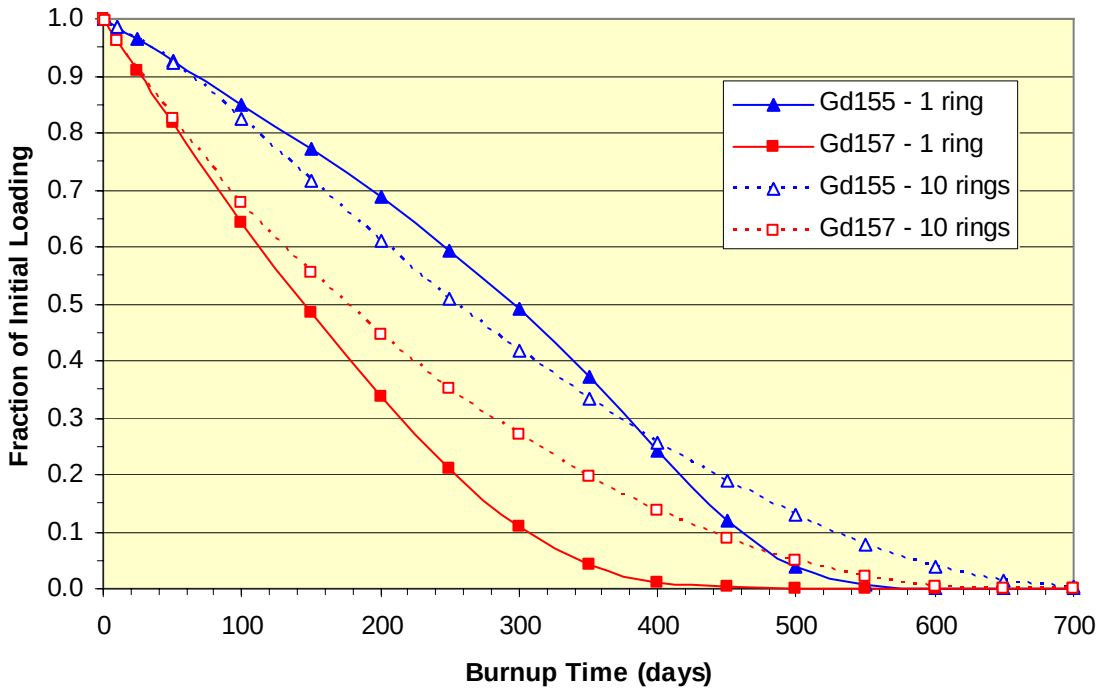

Figure 17. Total Gd in region 65 as a function of the spatial depletion representation

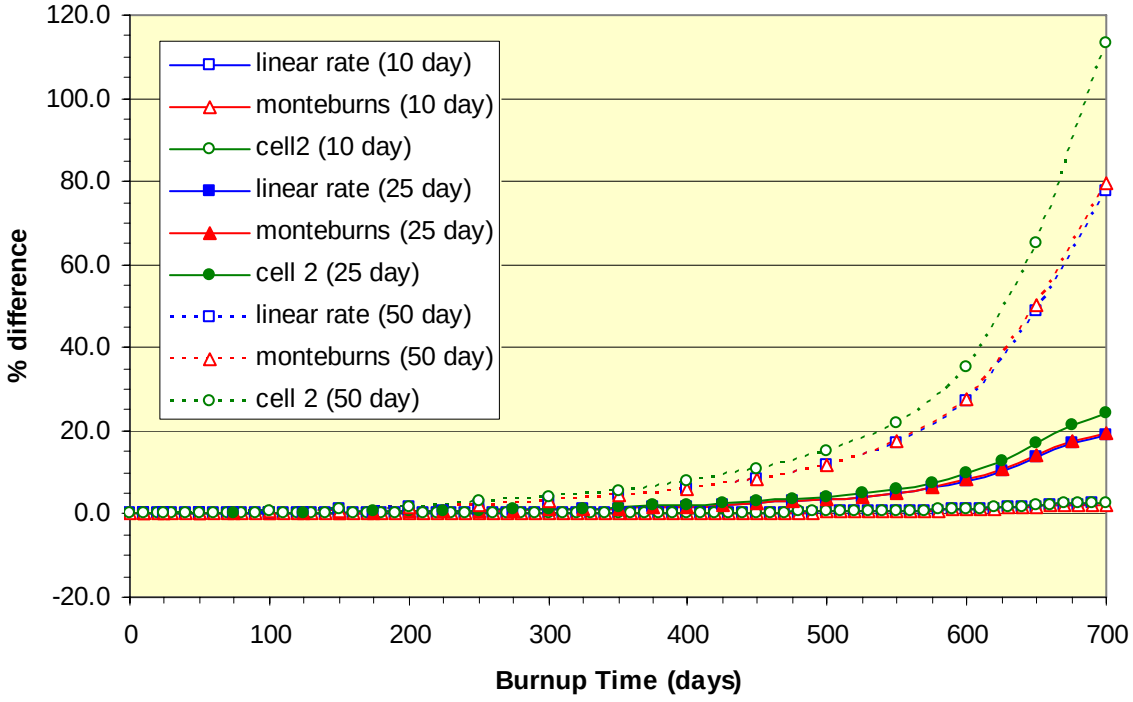

Figure 18. Percent difference in ^{155}Gd concentrations when using 10-region Gd-U fuel rods

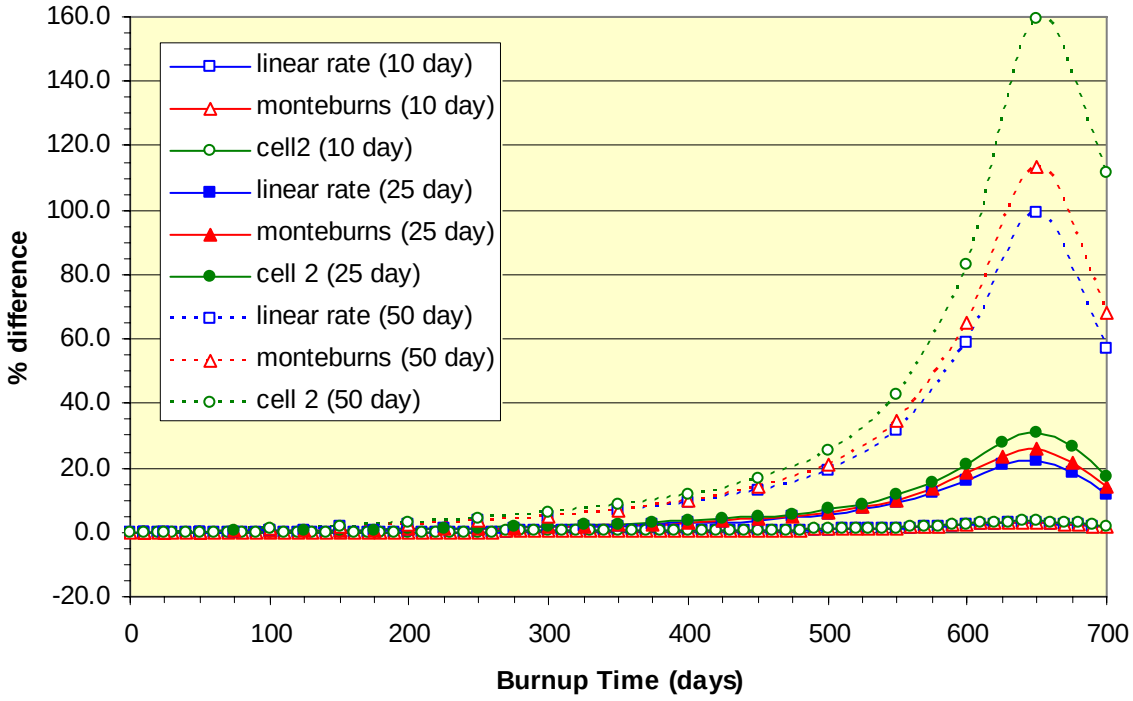

Figure 19. Percent difference in ^{157}Gd concentrations when using 10-region Gd-U fuel rods

7. ITERATING WITH THE *LINEAR RATE* METHOD

The preceding analysis using the *linear rate* method was based on using a single predictor-corrector step per depletion step. Within CMCDT, the user can elect to iterate on the predictor-corrector steps by specifying the maximum number of predictors to run per timestep. A convergence check is made based on the difference in the k_{eff} of the predictor and corrector spatials. If the magnitude of the difference between the k_{eff} values is less than the uncertainty of the difference, the iterations are terminated. Several depletions were run, each with a different number of predictor-corrector iterations per timestep. The maximum timestep size was 100 days and the Gd-U fuel rods were modeled with just one depletable region. Figure 21 demonstrates how the accuracy of the *linear rate* method will change, depending on the number of predictor-corrector iterations performed. Note that increasing the number of iterations does demonstrate convergence to a final solution; however, it is not guaranteed to be the correct solution. This result should not be surprising. The *linear rate* method forces the depletion reaction rates to be linear in time. For this example, the Gd reaction rates have an exponentially increasing trend up to around 450 days (see Figure 2). After that, the trend reverses. Forcing a converged linear behavior during the first 450 days will ensure that the Gd will deplete faster than it should, hence the rise in the k_{eff} difference. As the trend flips over, the linear behavior now will under-deplete the remaining gadolinium so that the concentrations get more in sync with the reference solution which is reflected in the k_{eff} difference falling back to zero.

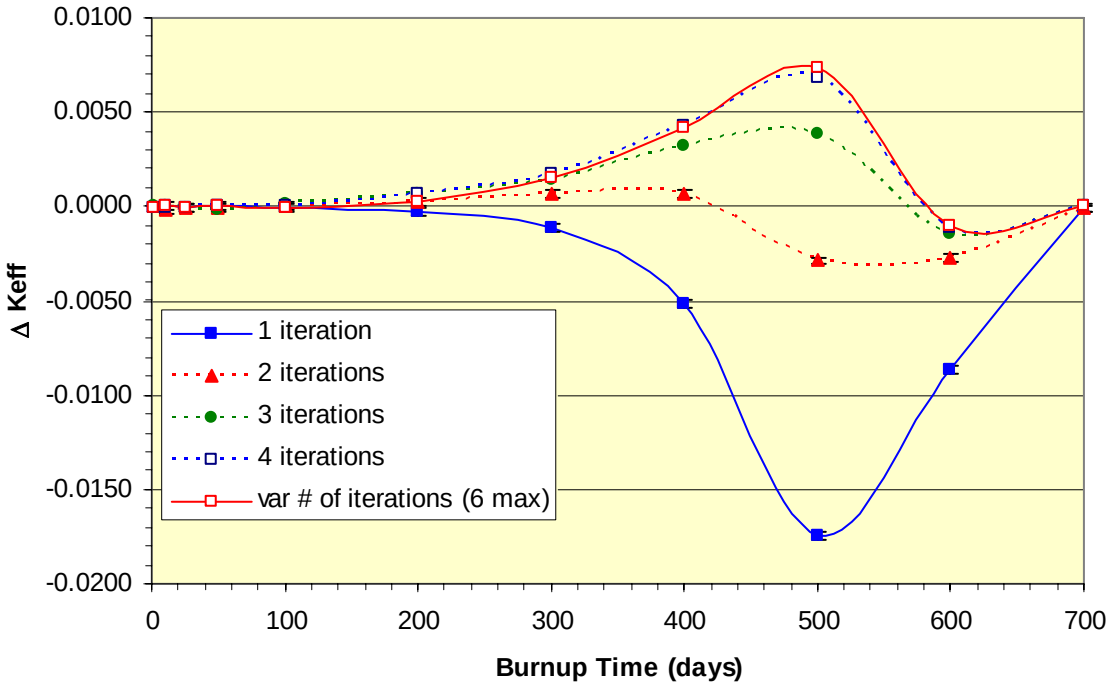

Figure 21. Change in keff as a result of iterating on the predictor-corrector steps

8. IMPROVING THE *LINEAR RATE* METHOD

As currently implemented in CMCDT, the slope calculations are simply the change between the BOT and EOT reaction rates divided by the length of the timestep. As is seen in Figure 2, such a straight forward approach is inaccurate due to the highly non-linear behavior in that reference frame. Instead of using time, the derivative can be based on differences in the logarithm of ratios of nuclide concentrations. Figure 20 shows how ^{155}Gd and ^{157}Gd reaction rates in rods 65 and 66 behave when plotted against the natural logarithm of their respective ratios of $N(0)/N(t)$. As can be seen, the trend is more linear than that observed in Figure 2.

Assuming a linear behavior, Equation (3) can be rewritten as

$$\mathbf{f}(t_s, \mathbf{y}_s) = \left[\mathbf{A}(t_0) + \mathbf{R}(\mathbf{y}_s)\right]\mathbf{y}_s \tag{4}$$

where

$$\mathbf{R}(\mathbf{y}_s) = \frac{\ln(\mathbf{y}_0 / \mathbf{y}_s)}{\ln(\mathbf{y}_0 / \tilde{\mathbf{y}}_1)}(\tilde{\mathbf{R}}_1 - \mathbf{R}_0) \tag{5}$$

Here, $\tilde{\mathbf{y}}_1$ and $\tilde{\mathbf{R}}_1$ are the solutions and reaction rates associated with predictor step depletion and EOT spatial based on those solutions. A similar technique has been employed successfully in Reference 7, although the underlying predictor-corrector method was based on the *cell2* approach and the derivatives used differences in the BOT and predictor number densities.

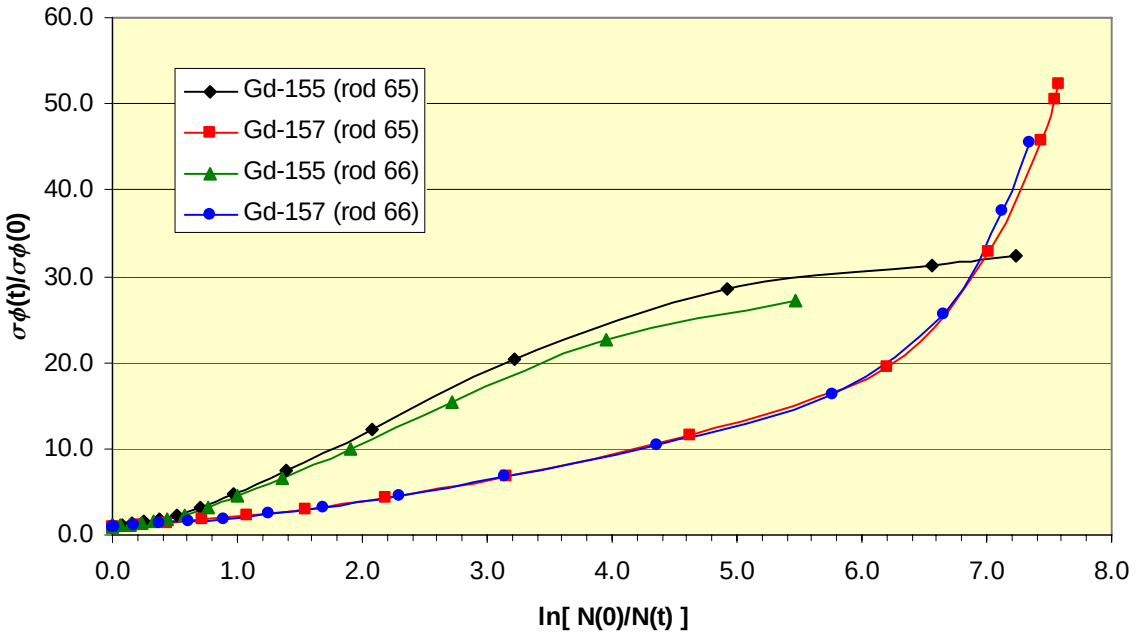

Figure 20. Relative change in gadolinium reaction rates as functions of the natural logarithm of concentration ratios

9. CONCLUSIONS

Using the CMCDT framework, a study has been done to assess three methods of implementing constant power depletion capability. The three methods are *cell2*, *monteburns* and *linear rate*. All three methods were run with various maximum size timesteps of 10, 25, 50 and 100 day intervals for a total depletion time of 700 days. The results were compared to a reference *linear rate* solution that used 5-day timestep intervals. All three methods demonstrate convergence to the reference solution as the timestep intervals become smaller. The *linear rate* method exhibited the best accuracy of all three methods, regardless of the timestep size. The *monteburns* method demonstrated close agreement to the linear rate method in many of the comparisons. Although the linear rate method can be used in an iterative fashion, the user is cautioned that the converged solution with coarse timesteps might not be the desired solution. Whereas the *cell2* and *monteburns* methods can be implemented independent of the underlying depletion solver, the *linear rate* method requires a solver that is capable of generating subinterval results such that the depletion coefficient matrix can be incrementally adjusted. ODE solvers are excellent candidates for such manipulations. For these results, there are no discernable differences in run time since the amount of time spent in depletion mode is negligible compared to the time running the spatial calculations. All three methods used the same number of spatial calculations. The *linear rate* method does require extra storage for the slope of the reaction rates. The *cell2* method requires storage for the solution of the second depletion in order to compute the average number densities. Although the *linear rate* methods results are good, the analysis indicates that an improved depletion algorithm could be obtained by switching the interpolant from time to a function of the logarithm of a nuclide's atom density. Such a change exhibits a more linear

behavior in the capture reaction rates for ^{155}Gd and ^{157}Gd which are critical to predicting accurate k_{eff} values.

REFERENCES

1. T. M. Sutton, *et al.*, "The MC21 Monte Carlo Transport Code," *Joint International Topical Meeting on Mathematics & Computation and Supercomputing in Nuclear Applications (M&C+SNA 2007),* Monterey, California, April 15-19, 2007, on CD-ROM
2. P. M. Brown, G. D. Byrne and A. C. Hindmarsh, "VODE: A Variable-Coefficient ODE Solver," *SIAM J. Sci. Stat. Comput.*, **10**, pp. 1038-1051 (1989)
3. C. M. Kang and R. O. Mosteller, "Incorporation of a Predictor-Corrector Depletion Capability into the CELL-2 Code," *Trans. Am. Nucl. Soc.*, **45**, pp 729-731, (1983)
4. D. I. Poston and H. R. Trellue, "Development of a Fully-Automated Monte Carlo Burnup Code MONTEBURNS," LA-UR-99-42, Los Alamos National Laboratory, January 1999
5. G. Marleau, A. Hebert, and R. Roy, "A User Guide for DRAGON Version4," IGE-294, Institut de genie nucleaire, Ecole Polytechnique de Montreal, July 16, 2008
6. A. Yamamoto, M. Tatsumi and N. Sugimura, "Projected Predictor-Corrector Method for Burnup Calculations of Gd-Bearing Fuel Assemblies," *International Conference on the Physics of Reactors(PHYSOR 2008),* Interlaken, Switzerland, September 14-19, 2008
7. A. Tamamoto, *et al.*, "Benchmark Problem Suite for Reactor Physics Study of LWR Next Generation Fuels," *J. Nucl. Sci. Technol.*, **39**, pp 900-912 (2002)
8. J. Hintze, NCSS and PASS, Number Cruncher Statistical Systems, Kaysville, UT, www.NCSS.com